Desalination and Water Treatment
www.deswater.com
doi: 10.1080/19443994.2016.1178177

57 (2016) 27783–27793
December

Taylor & Francis
Taylor & Francis Group

Kinetic studies for nitrate adsorption on granular chitosan–Fe(III) complex

Qili Hu[a,b], Nan Chen[a,b,*], Chuanping Feng[a,b], Weiwu Hu[c]

[a]*School of Water Resources and Environment, China University of Geosciences (Beijing), No. 29, Xueyuan Road, Haidian District, Beijing 100083, China, Tel. +86 18813181663; email: hustyle1234@163.com (Q. Hu), Tel. +86 13621327736; email: chennan@cugb.edu.cn (N. Chen), Tel. +86 10 82322281; email: fengcp@cugb.edu.cn (C. Feng)*
[b]*Key Laboratory of Groundwater Cycle and Environment Evolution, China University of Geosciences (Beijing), Ministry of Education, No. 29, Xueyuan Road, Haidian District, Beijing 100083, China*
[c]*The Journal Center, China University of Geosciences (Beijing), No. 29, Xueyuan Road, Haidian District, Beijing, China, Tel. +86 13811783404; email: hww2188@163.com*

Received 17 December 2015; Accepted 8 April 2016

ABSTRACT

In this study, a generalized kinetic equation was proposed to simulate adsorption behaviors in batch systems and several useful kinetic equations were deduced. The results indicated that the amount of nitrate uptake increased rapidly in the initial stage, followed by a slower process until adsorption equilibrium was reached after approximately 1.5 h. The rate constant was a function of the initial nitrate concentration. The adsorption and desorption rate constants quantitatively reflected the adsorption and desorption reactions at the solid/solution interface. The adsorption and desorption processes for nitrate adsorption followed identical reaction order. The kinetic parameters (adsorption and desorption rate constants, half-time and instantaneous rate) provided by these kinetic equations are of significant importance for the understanding of adsorption mechanisms.

Keywords: Nitrate adsorption; Chitosan; Kinetic models; Rate constant; Instantaneous rate; Half-time

1. Introduction

Adsorption is an attractive and promising technique for reducing pollutants in natural and industrial systems, contributing to addressing increasingly serious environmental and public problems [1,2]. Among various treatment techniques, adsorption has gained wide acceptance and popularity for the purification of municipal and industrial wastewaters due to its advantages of ease of operation, simplicity of design and low cost [3,4]. Study of adsorption kinetics is not only indispensable to the selection of suitable adsorbents, the design of adsorption systems and the analysis of investment costs [3], but it is also essential to predict kinetic parameters and provide useful information for explaining adsorption mechanisms [5].

Adsorption is generally regarded as a reversible two-way process in which an adsorbate spontaneously aggregates on the adsorbent surface through the solid/solution interface [6–8]. According to some generally expressed views, the adsorption process can be described by four consecutive kinetic steps, in which the lowest step is assumed to be the rate-determining step that controls the overall adsorption rate [9]. Intraparticle diffusion and surface reaction on the adsorbent surface are the primary rate-determining

*Corresponding author.

steps in the process of adsorption [10]. Moreover, Haerifar and Azizian reported that the intraparticle diffusion model was applicable when the rate-determining step was the mass transfer of adsorbate to adsorption sites on the adsorbent surface, while other models should be used for the description of adsorption kinetics when the overall adsorption rate was controlled by the rate of surface reaction [2]. Accordingly, it is exceedingly important to investigate kinetics and equilibrium in adsorption studies. Although various isotherm equations have been extensively reported, the theoretical basis of adsorption kinetics received less attention owing to the complexity of its theoretical description and the difficulty of establishing an adsorption equation for a given adsorption system [11].

The pseudo-first-order and pseudo-second-order kinetic equations [12,13] proposed as empirical models have been successfully utilized to describe the adsorption kinetics at the solid/solution interface due to the simplicity of mathematical expressions and their good fit with experimental results. It should be noted that the use of them requires the assumption that the rate of the adsorption chemical reaction controls the overall adsorption kinetics [2], which is intuitively connected with the corresponding one-site and two-site occupancy adsorption kinetic models governed by the rate of the surface reaction [14]. However, these two equations failed to provide the adsorption and desorption rate constants. Consequently, to describe adsorption and desorption behaviors at the solid/solution interface, kinetic models that represent the time dependency of the adsorption and desorption processes should be developed.

In the present study, the theoretical basis and application conditions of three traditional kinetic equations were first analyzed. A generalized kinetic equation was proposed and some derived kinetic equations with exact analytical solutions were employed to fit with the experimental data. The feasibility of these novel kinetic models was investigated by analyzing the kinetics of nitrate adsorption on granular chitosan–Fe(III) complex.

2. Materials and methods

2.1. Materials

In this study, the various required concentrations of nitrate solution were prepared with deionized water. All of the chemicals were used as received and are listed in Table 1.

2.2. Adsorbent synthesis

A certain amount of ferric chloride was added to a beaker containing 300 mL of deionized water and then continuously stirred at room temperature for 20 min. The pH value of $FeCl_3$ solution was 1.78. Subsequently, 10 g of chitosan powder was adequately dissolved in $FeCl_3$ solution for 2.0 h. Chitosan–Fe(III) hydrogel beads were prepared by dropwise addition of this chitosan solution to an alkaline coagulating mixture (H_2O:$NH_3{\cdot}H_2O$:CH_3CH_2OH 3:2:1, v/v). After being stabilized for 1.0 h, the hydrogel beads were separated, sufficiently washed with deionized water, and then dried at 50˚C for 8.0 h in an oven. The dried beads were immersed in deionized water at 50˚C for 4.0 h in a horizontal shaker. After separation, washing, and drying, granular chitosan–Fe(III) complex was obtained.

2.3. Kinetic experiments

One hundred milliliters of nitrate solution (20, 40, 60, 80, and 100 mg L^{-1} (as N)) was poured into 250-mL conical flasks containing adsorbent (2.0 g), which were then agitated at 120 rpm and 20˚C in a thermostatic shaker. One milliliter of the sample solution was taken from these conical flasks at certain time intervals to analyze the residual nitrate concentration. The kinetic experiments for each initial nitrate concentration were performed in duplicate to obtain better accuracy.

The amount of nitrate adsorbed per unit mass of adsorbent was calculated at time t using the following equation [15]:

$$q_t = \frac{(C_0 - C_t) \times V}{M} \tag{1}$$

where q_t (mg g^{-1}) is the amount of nitrate nitrogen adsorbed at time t; C_0 (mg L^{-1}) and C_t (mg L^{-1}) are the nitrate nitrogen concentrations at the initial time and at time t, respectively; V (L) is the working volume; and M (g) is the mass of adsorbent used.

2.4. Analysis

The concentration of nitrate was measured though a standard colorimetric method using a UV/vis spectrophotometer (DR 6000, HACH, USA) with a minimum detectable concentration of 0.08 mg L^{-1} (as N). The pH value was determined using a pH meter (SevenMulti S40, METTLER-TOLEDO, Switzerland).

Table 1
Chemicals used in this study

Chemicals	Molecular formula	Molecular weight	CAS no.	Source	Assay (%)	Grade
Chitosan	$(C_6H_{11}NO_4)_n$	161.2n	9012-76-4	Sinopharm Chemical Reagent Co., Ltd	80–90	BR
Ferric chloride	$FeCl_3{\cdot}6H_2O$	270.29	7705-08-0	Tianjin Fuchen Chemical Reagents Factory	99.0	AR
Ammonia solution	NH_3	17.03	1336-21-6	Beijing Chemical Works	25	AR
Ethanol	C_2H_6O	46.07	64-17-5	Beijing Chemical Works	99.5	AR
Potassium nitrate	KNO_3	101.10	7784-27-2	Beijing Chemical Works	99.0	AR
Sulfamic acid	H_3NO_3S	97.09	5329-14-6	Shanghai Zhanyun Chemical Co., Ltd	99.5	AR
Hydrochloric acid	HCl	36.46	7647-01-0	Beijing Chemical Works	36–38	AR

3. Theoretical analysis

3.1. Adsorption kinetics

It is generally considered that adsorption and desorption occur simultaneously at the solid/solution interface. The solute concentration in aqueous solution remains constant when the adsorption equilibrium appears. It should be assumed that residual solute at equilibrium fails to participate in adsorption reaction. In adsorption studies, it is difficult to predict the order of the overall reaction, which is attributed to the fact that adsorption is an extremely complex process involving various adsorption mechanisms such as electrostatic attraction, ion exchange, external or internal mass transfers, and surface reactions [16,17].

Based on the above analysis, to more accurately forecast the variation trend of solute uptake with time, the differential form of the pseudo-nth-order kinetic equation was defined as follows [18]:

$$\frac{dq_t}{dt} = k_n(q_e - q_t)^n \tag{2}$$

where q_e (mg g^{-1}) and q_t (mg g^{-1}) are the amounts of solute adsorbed per unit mass of adsorbent at equilibrium and at time t, respectively; k_n (g^{n-1} mg^{1-n} min^{-1}) is the pseudo-nth-order rate constant; n ($n \neq 1$) stands for the order of the whole reaction, which was a real number; and t (min) is the contact time. The integrated form of Eq. (2) at the boundary conditions $t = 0$ to $t = t$ and $q_t = 0$ to $q_t = q_t$ is given as follows:

$$q_t = q_e\left[1 - \left(\frac{1}{1 + k_n(n-1)q_e^{n-1}t}\right)^{\frac{1}{n-1}}\right] \tag{3}$$

In particular, when the adsorption process obeyed first-order and second-order kinetics, two widely used kinetic equations could be obtained from Eq. (3), which are the so-called pseudo-first-order and pseudo-second-order kinetic equations. Substituting $n = 1$ and $n = 2$ into Eq. (2), the integrated forms of the pseudo-first-order and pseudo-second-order kinetic equations are given as follows:

$$q_t = q_e\left[1 - \exp(-k_1 t)\right] \tag{4}$$

$$q_t = q_e\left(1 - \frac{1}{1 + k_2 q_e t}\right) \tag{5}$$

where k_1 (min^{-1}) and k_2 (g mg^{-1} min^{-1}) are the pseudo-first-order and pseudo-second-order rate constants, respectively.

It is not difficult to find that the above kinetic equations can be employed to describe a reversible adsorption/desorption process. This partly explains why these kinetic equations have been widely used to describe adsorption reactions at the solid/solution interface since they were proposed. Marczewski reported that the pseudo-first-order kinetic equation could describe typical diffusion-dependent kinetics [19]. According to Karadag et al., if the adsorption rate was controlled by chemical exchange, the pseudo-second-order kinetic equation was well fitted with the experimental data [20]. Furthermore, as suggested by Rudzinski and Plazinski, the pseudo-first-order and pseudo-second-order kinetic equations may describe adsorption systems with highly heterogeneous solid surfaces [14].

3.2. Modification of adsorption kinetics

Adsorption kinetics is typically characterized by a diffusion-dependent process in which the concentration gradient as a driving force overcome mass transfer resistance at the solid/liquid interface [21]. Kinetic equations are primarily employed to obtain several important kinetic parameters and provide useful information for adsorption mechanisms. Therefore, it is extremely essential to establish an equation that can simultaneously describe adsorption and desorption behaviors at the solid/solution interface.

The pseudo-first-order and pseudo-second-order kinetic equations have been widely employed to describe kinetic data obtained under non-equilibrium conditions in recent years [7]. Their success undoubtedly reflects their ability to fit a wide variety of kinetic data quite well, but it may also partly reflect the appealing simplicity of the kinetic equations. Nevertheless, these equations did not give the adsorption and desorption rate constants or account for the factors influencing equilibrium solute uptake. Thus, it is difficult to know the extent of adsorption reactions and how to optimize experimental conditions to promote equilibrium solute uptake. As a result, it is exceedingly necessary to modify the above adsorption kinetic equations.

To establish more reasonable kinetic models and analyze the theoretical basis of the kinetic equations, the initial content of solute in aqueous solution was converted to the amount of solute per unit mass of adsorbent, which was defined as follows:

$$Q = \frac{C_0 \times V}{M} \tag{6}$$

where Q (mg g^{-1}) is a constant for a given adsorption system.

Based on the above analysis, a generalized kinetic equation was first proposed, which was defined as follows:

$$\frac{dq_t}{dt} = k_a(Q - q_t)^{n_1} - k_d q_t^{n_2} \tag{7}$$

where k_a and k_d are the adsorption and desorption rate constants, respectively; and n_1 and n_2 are the orders of adsorption and desorption reactions, respectively.

Several useful equations can be obtained from Eq. (7) despite the fact that this equation fails to provide an analytical solution.

If $n_1 = 1$ and $n_2 = 1$, the integrated form of kinetic model I is expressed as follows:

$$q_t = \frac{k_a Q}{k_a + k_d}\{1 - \exp[-(k_a + k_d)t]\} \tag{8}$$

If $n_1 = 2$ and $n_2 = 2$, the integrated form of kinetic model II is expressed as follows:

$$q_t = \frac{k_a Q}{k_a - k_d} - \frac{Q\sqrt{k_a k_d}}{k_a - k_d}\left[1 - \frac{2}{1 - \frac{\sqrt{k_a}+\sqrt{k_d}}{\sqrt{k_a}-\sqrt{k_d}}\exp\left(2Q\sqrt{k_a k_d}t\right)}\right] \tag{9}$$

If $n_1 = 1$ and $n_2 = 2$, the integrated form of kinetic model III is expressed as follows:

$$q_t = -\frac{k_a}{2k_d} + \frac{\sqrt{4k_a k_d Q + k_a^2}}{2k_d} \times \left[1 - \frac{2}{1 - \frac{k_a+\sqrt{4k_a k_d Q+k_a^2}}{k_a-\sqrt{4k_a k_d Q+k_a^2}}\exp\left(\sqrt{4k_a k_d Q + k_a^2}t\right)}\right] \tag{10}$$

If $n_1 = 2$ and $n_2 = 1$, the integrated form of kinetic model IV is expressed as follows:

$$q_t = Q + \frac{k_d}{2k_a} - \frac{\sqrt{4k_a k_d Q + k_d^2}}{2k_a} \times \left[1 - \frac{2}{1 - \frac{2k_a Q+k_d+\sqrt{4k_a k_d Q+k_d^2}}{2k_a Q+k_d-\sqrt{4k_a k_d Q+k_d^2}}\exp\left(\sqrt{4k_a k_d Q + k_d^2}t\right)}\right] \tag{11}$$

Adsorption and desorption rate constants can be obtained from the nonlinear fitting curve of q_t vs. t, while the calculation of equilibrium solute uptake and the zero-order reaction can be found in the Supplementary materials. It should be mentioned that the proposed novel kinetic models include a time-dependent exponential term, implying that solute uptake exponentially approaches a limiting value in the batch system. Therefore, adsorption occurs rapidly in the initial stage, followed by a slow step until equilibrium. The adsorption process primarily consists of three steps [8,16,22]: (i) diffusion through boundary layer around the sorbent to access the adsorbent

surface (film diffusion); (ii) diffusion along the adsorbent pores to access the active sites (intraparticle diffusion); and (iii) adsorbate adsorption on the active sites (physisorption or chemisorption).

4. Results and discussion

4.1. Adsorption performance

Contact time and initial solute concentration are two vital factors influencing equilibrium solute uptake and effluent concentration for a given adsorption system. As illustrated in Fig. 1, it was observed that the amount of nitrate adsorbed increased rapidly in the first 20 min, followed by a slower process until adsorption equilibrium was reached after approximately 1.5 h for each initial nitrate concentration. This meant that nitrate adsorption on the granular chitosan–Fe(III) complex was typical of the specific adsorption process in which the adsorption rate is normally dependent upon the number of available adsorption sites on the adsorbent surface and is eventually controlled by the attachment of nitrate ions on the surface [23,24]. Moreover, as shown in Table 2, the amount of nitrate adsorbed at equilibrium was found to increase with the increase in initial nitrate concentration. This behavior was ascribed to the fact that the increase in the number of nitrate ions induced a shift of the adsorption equilibrium toward favorable adsorption. However, the limited adsorption sites fail to accommodate nitrate ions at high concentration for a certain amount of adsorbent, leading to an increase in the effluent concentration. Consequently, identifying the ratio of initial nitrate concentration to adsorbent dosage is of extreme significance for achieving high adsorption capacity and low effluent concentration.

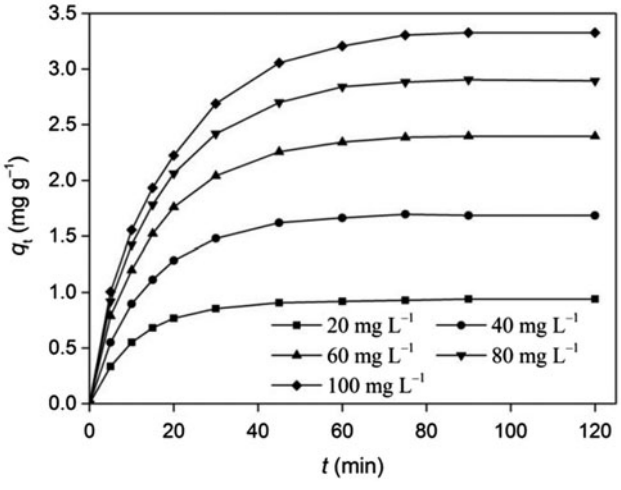

Fig. 1. The effects of contact time and initial nitrate concentration on nitrate removal.

4.2. Comparison of various kinetic equations

In the present study, the coefficient of determination (R^2) [25] and chi-square analysis (χ^2) [26] were utilized to evaluate the goodness of fit of various kinetic equations to the experimental data and were defined as follows:

$$R^2 = \frac{\sum(q_{cal} - \bar{q}_t)^2}{\sum(q_{cal} - \bar{q}_t)^2 + \sum(q_{cal} - q_{exp})^2} \quad (12)$$

$$\chi^2 = \sum \frac{(q_{exp} - q_{cal})^2}{q_{cal}} \quad (13)$$

where q_{exp} (mg g^{-1}) is the experimental nitrate uptake at time t; q_{cal} (mg g^{-1}) is the calculated nitrate uptake; and $\overline{q_t}$ (mg g^{-1}) is the average value of q_{exp}.

It can be clearly seen from Fig. 2 that the three traditional kinetic models are fitted well with the experimental data. Similar results were found for other initial nitrate nitrogen concentrations (data not shown). However, there were some subtle differences between these fitting results. As shown in Table 2, compared with the pseudo-second-order kinetic model, the pseudo-first-order kinetic model provided equilibrium nitrate uptake closer to the experimental nitrate uptake for each initial nitrate concentration. The pseudo-*n*th-order kinetic model had the highest coefficient of determination value and the lowest chi-square value. Moreover, the order of the overall reaction obtained from the pseudo-*n*th-order kinetic model was a non-integer (near 1) for each initial nitrate concentration, indicating that nitrate adsorption on granular chitosan–Fe(III) complex is an extremely complicated process that obeys the pseudo-first-order kinetic model. It should be stressed that the pseudo-*n*th-order kinetic model was independent of the order of the overall reaction and thereby provided better correlation between the fitting results and the experimental data.

It can be observed from Fig. 3 that the novel kinetic models provided good correlation for the experimental data. Similar results were obtained for other initial nitrate concentrations (data not shown). As detailed in Table 3, the value of the coefficient of determination was higher than 0.99 and the chi-square value was lower than 0.01 for each nitrate concentration when using these kinetic models, suggesting that these kinetic models were fitted well with the

Table 2
Kinetic parameters obtained from pseudo-first-order, pseudo-second-order, and pseudo-*n*th-order kinetic models

C_0 (mg L^{-1})	q_{exp} (mg g^{-1})	q_{cal} (mg g^{-1})	k_1 (min^{-1})	R^2	χ^2
Pseudo-first-order kinetic model					
20	0.939	0.930	8.79×10^{-2}	0.9995	4.96×10^{-5}
40	1.685	1.684	7.37×10^{-2}	0.9992	2.73×10^{-4}
60	2.397	2.383	6.90×10^{-2}	0.9980	1.38×10^{-3}
80	2.894	2.884	6.54×10^{-2}	0.9975	2.54×10^{-3}
100	3.326	3.311	5.94×10^{-2}	0.9964	4.71×10^{-3}
C_0 (mg L^{-1})		q_{cal} (mg g^{-1})	k_2 (g mg^{-1} min^{-1})	R^2	χ^2
Pseudo-second-order kinetic model					
20		1.046	0.1124	0.9912	9.09×10^{-4}
40		1.926	4.84×10^{-2}	0.9926	2.56×10^{-3}
60		2.745	3.11×10^{-2}	0.9950	3.48×10^{-3}
80		3.344	2.38×10^{-2}	0.9955	4.62×10^{-3}
100		3.884	1.80×10^{-2}	0.9959	5.58×10^{-3}
C_0 (mg L^{-1})	q_{cal} (mg g^{-1})	n	k_n (g^{n-1} mg^{1-n} min^{-1})	R^2	χ^2
Pseudo-*n*th-order kinetic model					
20	0.940	1.104	9.29×10^{-2}	0.9999	1.72×10^{-5}
40	1.701	1.121	7.27×10^{-2}	0.9996	1.38×10^{-4}
60	2.439	1.225	6.13×10^{-2}	0.9992	5.90×10^{-4}
80	2.968	1.256	5.40×10^{-2}	0.9990	1.15×10^{-3}
100	3.445	1.308	4.44×10^{-2}	0.9983	2.57×10^{-3}

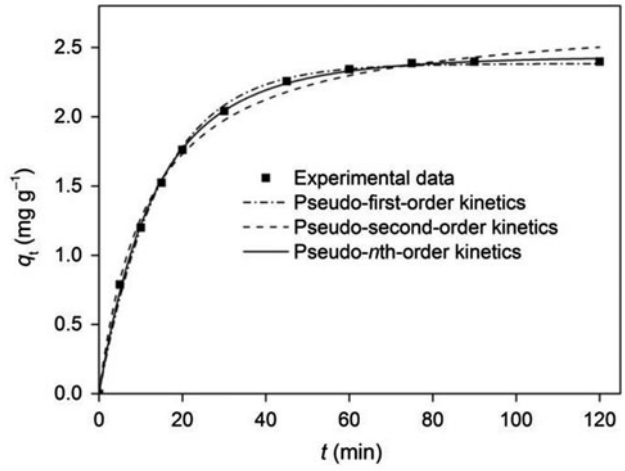

Fig. 2. Kinetic studies of nitrate removal with an initial concentration of 60 mg L^{-1} (as N).

experimental data. Kinetic model I is superior to the pseudo-first-order kinetic model because kinetic model I provides adsorption and desorption rate constants that are beneficial to understanding the interfacial process in the batch system. Compared with the pseudo-second-order kinetic model, kinetic model II not only had a higher coefficient of determination value and a lower chi-square value for each initial nitrate concentration, but it also provided an equilibrium nitrate uptake closer to the experimental nitrate uptake. Kinetic model I and kinetic model II are superior to kinetic model III and kinetic model IV, respectively, from the viewpoint of nitrate uptake, indicating that the adsorption and desorption processes for nitrate adsorption on granular chitosan–Fe(III) complex followed identical reaction order. It should be noted that kinetic model I was the most suitable for describing nitrate adsorption because the fitting result (q_{cal}) was closest to the experimental data (q_{exp}) among four the new kinetic models.

4.3. Half-time

In the present study, half-time was proposed as a better reflection of the variation trend of nitrate uptake with time. Half-time is defined as the time required for the amount of nitrate ions to decease by half (see the Supplementary materials). As illustrated in Table 3, the value of the half-time increased significantly with the increase in initial nitrate concentration. It is not difficult to understand that large amounts of available adsorption sites adsorb nitrate ions at low concentrations, resulting in short half-time and high removal efficiency. However, the adsorption sites are not sufficient enough to accommodate continuously

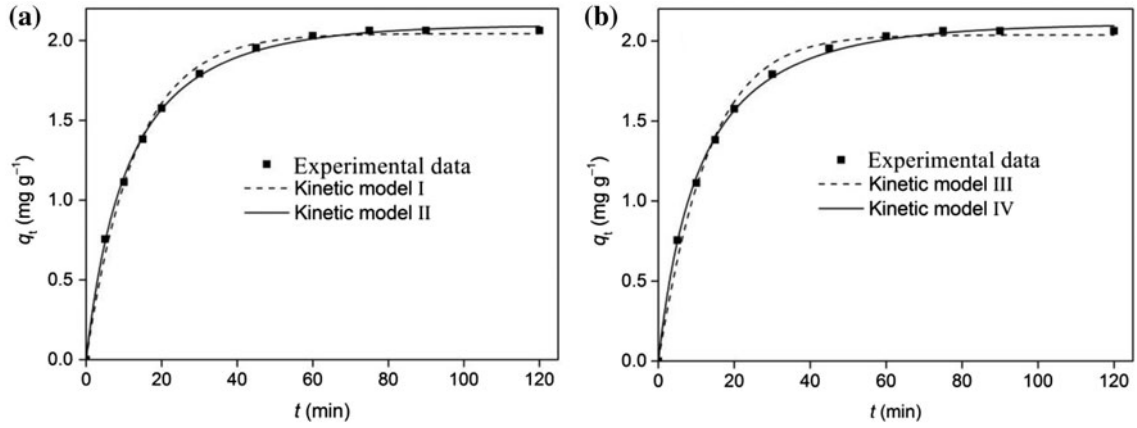

Fig. 3. Kinetic studies of nitrate removal with an initial concentration of 60 mg L^{-1} (as N): (a) kinetic model I and kinetic model II and (b) kinetic model III and kinetic model IV.

Table 3
Kinetic parameters obtained from kinetic model I, kinetic model II, kinetic model III, and kinetic model IV

C_0 (mg L^{-1})	q_{cal} (mg g^{-1})	k_a (min^{-1})	k_d (min^{-1})	T (min)	R^2	χ^2
Kinetic model I						
20	0.930	7.89×10^{-2}	9.01×10^{-3}	9.27	0.9995	4.96×10^{-5}
40	1.684	6.05×10^{-2}	1.32×10^{-2}	12.74	0.9992	2.73×10^{-4}
60	2.383	5.16×10^{-2}	1.74×10^{-2}	15.99	0.9980	1.38×10^{-3}
80	2.884	4.48×10^{-2}	2.06×10^{-2}	20.04	0.9975	2.54×10^{-3}
100	3.310	3.76×10^{-2}	2.18×10^{-2}	26.35	0.9964	4.71×10^{-3}
C_0 (mg L^{-1})	q_{cal} (mg g^{-1})	k_a (g mg^{-1} min^{-1})	k_d (g mg^{-1} min^{-1})	T (min)	R^2	χ^2
Kinetic model II						
20	0.991	0.1184	2.43×10^{-4}	8.16	0.9912	9.13×10^{-4}
40	1.742	4.03×10^{-2}	1.27×10^{-3}	12.21	0.9965	1.24×10^{-3}
60	2.439	2.02×10^{-2}	1.89×10^{-3}	16.05	0.9992	5.58×10^{-4}
80	2.931	1.24×10^{-2}	2.36×10^{-3}	20.55	0.9994	6.12×10^{-4}
100	3.352	0.79×10^{-2}	2.51×10^{-3}	27.21	0.9984	2.15×10^{-3}
C_0 (mg L^{-1})	q_{cal} (mg g^{-1})	k_a (min^{-1})	k_d (g mg^{-1} min^{-1})	T (min)	R^2	χ^2
Kinetic model III						
20	0.929	7.59×10^{-2}	9.47×10^{-3}	9.33	0.9992	8.13×10^{-5}
40	1.679	5.68×10^{-2}	7.50×10^{-3}	12.80	0.9983	5.89×10^{-4}
60	2.371	4.74×10^{-2}	6.85×10^{-3}	15.93	0.9961	2.74×10^{-3}
80	2.866	4.03×10^{-2}	6.59×10^{-3}	19.69	0.9947	5.40×10^{-3}
100	3.283	3.33×10^{-2}	6.04×10^{-3}	25.45	0.9929	9.65×10^{-3}
C_0 (mg L^{-1})	q_{cal} (mg g^{-1})	k_a (g mg^{-1} min^{-1})	k_d (min^{-1})	T (min)	R^2	χ^2
Kinetic model IV						
20	0.998	0.1183	1.74×10^{-4}	8.17	0.9911	9.20×10^{-4}
40	1.751	4.08×10^{-2}	2.10×10^{-3}	12.20	0.9960	1.41×10^{-3}
60	2.452	2.08×10^{-2}	4.55×10^{-3}	16.05	0.9988	8.21×10^{-4}
80	2.950	1.29×10^{-2}	6.97×10^{-3}	20.69	0.9993	6.97×10^{-4}
100	3.379	8.40×10^{-3}	8.58×10^{-3}	27.69	0.9988	1.63×10^{-3}

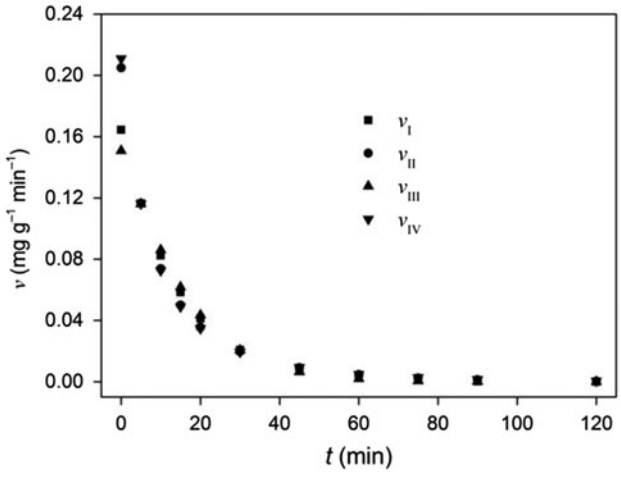

Fig. 4. The plot of instantaneous rate vs. initial nitrate concentration (60 mg L^{-1}, as N).

increasing nitrate ions for a certain amount of adsorbent at high concentration, leading to long half-time and low removal efficiency. Obviously, controlling the ratio of initial nitrate concentration to adsorbent dosage is essential to shorten half-time. Moreover, identifying the half-time of an adsorption process is of prime importance for the design of a practical adsorption system. For example, according to the requirement of process design, when nitrate removal efficiency reaches a preset value, the treatment time (t) required can be calculated using the following equation:

$$t = 2\omega T \tag{14}$$

where ω (%) is the preset removal efficiency; and T (min) is the optimal fitting half-time.

4.4. Instantaneous rate

Instantaneous rate is also a crucial parameter reflecting the changing rate of solute uptake at a given time. To the best of our knowledge, in previous studies, there have been no reports about instantaneous rate of solute uptake with time.

As depicted in Fig. 4, the instantaneous rate decreased rapidly in the first 20 min, followed by a slow process and a slight fluctuation after around 1.0 h. This result is exactly opposite to the variation trend of equilibrium nitrate uptake with time. Similar results were observed for other initial nitrate nitrogen concentrations (Supplementary Materials, Fig. A1). The instantaneous rate increased with the increase in initial nitrate concentration at any time (Supplementary Materials, Table A1). This partly explains equilibrium nitrate uptake increased with the increase in initial nitrate concentration. In the present study, the initial

Table 4
Fitting instantaneous rate parameters obtained from the simple exponential function

C_0 (mg L^{-1})	Kinetic model	a	b	R^2	χ^2
20	I	0.0817	0.0879	1.0000	5.227×10^{-20}
	II	0.1252	0.1636	0.9901	1.570×10^{-5}
	III	0.0792	0.0837	0.9997	2.415×10^{-7}
	IV	0.1251	0.1635	0.9901	1.578×10^{-5}
40	I	0.1241	0.0737	1.0000	1.268×10^{-19}
	II	0.1658	0.1156	0.9908	2.734×10^{-5}
	III	0.1181	0.0680	0.9990	1.801×10^{-6}
	IV	0.1678	0.1177	0.9904	2.916×10^{-5}
60	I	0.1645	0.0690	1.0000	6.081×10^{-20}
	II	0.2001	0.0946	0.9934	2.993×10^{-5}
	III	0.1541	0.0619	0.9980	6.359×10^{-7}
	IV	0.2057	0.0987	0.9923	3.661×10^{-5}
80	I	0.1885	0.0654	1.0000	8.972×10^{-20}
	II	0.2149	0.0811	0.9959	2.229×10^{-5}
	III	0.1745	0.0573	0.9968	1.324×10^{-5}
	IV	0.2238	0.0866	0.9940	3.449×10^{-5}
100	I	0.1966	0.0594	1.0000	6.554×10^{-20}
	II	0.2137	0.0684	0.9977	1.303×10^{-5}
	III	0.1809	0.0514	0.9954	2.061×10^{-5}
	IV	0.2248	0.0744	0.9953	2.857×10^{-5}

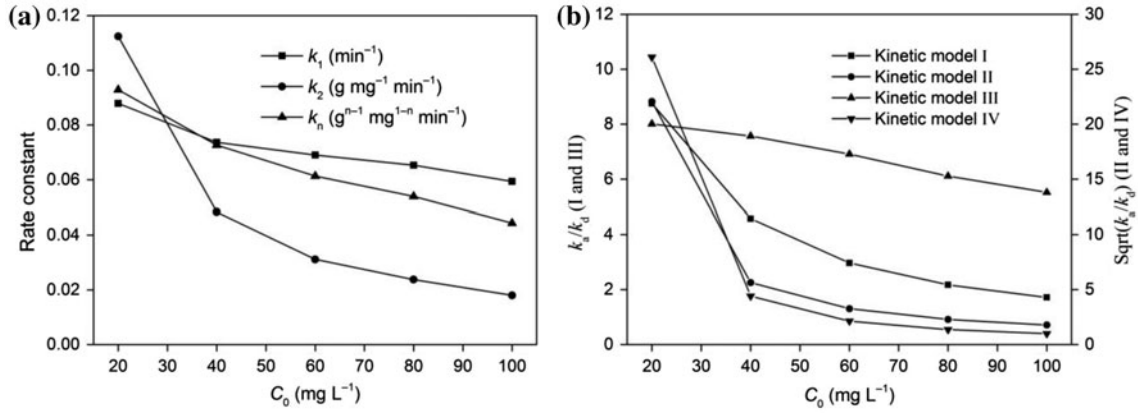

Fig. 5. The effects of initial nitrate concentration on rate constants: (a) k_1, k_2 and k_n; (b) k_a and k_d.

adsorption rates obtained from kinetic model I were found to be 8.174×10^{-2} mg g^{-1} min^{-1} for 20 mg L^{-1}, 0.1241 mg g^{-1} min^{-1} for 40 mg L^{-1}, 0.1645 mg g^{-1} min^{-1} for 60 mg L^{-1}, 0.1885 mg g^{-1} min^{-1} for 80 mg L^{-1}, and 0.1966 mg g^{-1} min^{-1} for 100 mg L^{-1}. In addition, instantaneous rates obtained from kinetic model I, kinetic model II, kinetic model III, and kinetic model IV had identical variation tends and the differences between them were very small. The instantaneous rate has an exceedingly complicated mathematical expression that contains a time-dependent exponent term. Hence, a simple exponential function is proposed to describe instantaneous rate, which was expressed as follows:

$$v = a \cdot \exp(-b \cdot t) \tag{15}$$

where a and b are the empirical coefficient.

It can be observed from Table 4 that the value of coefficient of determination was higher than 0.99 and the chi-square value was lower than 3.7×10^{-5} for each initial nitrate concentration among these kinetic models, suggesting that this simple exponential equation also describes instantaneous rate with great accuracy ignoring complicated mathematical expressions. It should be noted that the value of coefficient of determination is 1.00 when Eq. (15) is fitted with the instantaneous rate obtained from kinetic model I due to the identical mathematical forms.

4.5. Rate constants

This section investigates the effect of initial nitrate concentration on the rate constants. As shown in Table 2, the values of the rate constants (k_1, k_2, and k_n) decreased with decreasing initial nitrate concentration. In fact, larger rate constants required shorter times to reach a specific removal efficiency relative to smaller rate constants [27]. Therefore, an adsorption system with a lower concentration can rapidly reach a specific removal efficiency. This result was in agreement with our study where the shorter half-time were observed at low concentration. As shown in Fig. 5(a), compared with the pseudo-second-order rate constant, the pseudo-nth-order rate constant was closer to the pseudo-first-order rate constant, which indirectly indicated that nitrate adsorption on granular chitosan–Fe (III) complex obeyed the pseudo-first-order kinetic model.

It can be clearly seen from Table 3 that all of the adsorption rate constants decreased with the increase in initial nitrate concentration, while the desorption rate constants increased except for that of kinetic model III. This result indicates that nitrate desorption on the granular chitosan–Fe(III) complex did not follow second order reaction kinetics. Therefore, kinetic model III is not suitable for describing nitrate adsorption. As illustrated in Fig. 5(b), the ratio of k_a to k_d for kinetic model I and kinetic model II or the square root of k_a to k_d for kinetic model III and kinetic model IV shared a downward trend with the increase in initial nitrate concentration. Thus, the occurrence of the adsorption reaction was feasible and favorable.

5. Conclusions

The present study demonstrated that granular chitosan–Fe(III) complex is an effective adsorbent for the removal of nitrate from aqueous solution. The rate of adsorption of nitrate on granular chitosan–Fe(III) complex increased rapidly in the initial stage, followed by a slow process until adsorption equilibrium was reached. A proper ratio of initial nitrate concentration to adsorbent dosage is essential to shorten the half-time. The rate constant is a function of the initial

nitrate concentration. These kinetic equations are in good agreement with the experimental data. Three traditional kinetic equations shared simple mathematical expressions and the pseudo-*n*th-order kinetic model was independent of the order of the overall reaction. In this study, kinetic parameters (adsorption and desorption rate constants, half-time and instantaneous rate) provided by the novel kinetic equations are of extreme significance for understanding adsorption mechanisms and optimizing adsorption systems. Moreover, these novel kinetic models are probably suitable for the adsorption of a particular solute on various adsorbents or the adsorption of various solutes on a particular adsorbent because the two modified kinetic models did not limit the types of solutes or adsorbents in theory analysis. These results will be validated by a series of adsorption experiments in future studies.

Supplementary material

The supplementary material for this paper is available online at http://dx.doi.10.1080/19443994.2016.1178177.

Acknowledgments

The authors acknowledge financial supports from the National Natural Science Foundation of China (NSFC) (No. 21407129; No. 41401545) and the Fundamental Research Funds for the Central Universities (No. 2652015121).

References

[1] S. Azizian, H. Bashiri, Description of desorption kinetics at the solid/solution interface based on the statistical rate theory, Langmuir 24 (2008) 13013–13018.
[2] M. Haerifar, S. Azizian, Mixed surface reaction and diffusion-controlled kinetic model for adsorption at the solid/solution interface, J. Phys. Chem. C 117 (2013) 8310–8317.
[3] S. Azizian, M. Haerifar, J. Basiri-Parsa, Extended geometric method: A simple approach to derive adsorption rate constants of Langmuir-Freundlich kinetics, Chemosphere 68 (2007) 2040–2046.
[4] P. Loganathan, S. Vigneswaran, J. Kandasamy, Enhanced removal of nitrate from water using surface modification of adsorbents—A review, J. Environ. Manage. 131 (2013) 363–374.
[5] M. Haerifar, S. Azizian, Fractal-like adsorption kinetics at the solid/solution interface, J. Phys. Chem. C 116 (2012) 13111–13119.
[6] I. Langmuir, The adsorption of gases on plane surfaces of glass, mica and platinum, J. Am. Chem. Soc. 40 (1918) 1361–1403.
[7] Y. Liu, L. Shen, From Langmuir kinetics to first- and Second-Order rate equations for adsorption, Langmuir 24 (2008) 11625–11630.
[8] C. Tien, B.V. Ramarao, Further examination of the relationship between the Langmuir kinetics and the Lagergren and the second-order rate models of batch adsorption, Sep. Purif. Technol. 136 (2014) 303–308.
[9] W. Rudzinski, W. Plazinski, Theoretical description of the kinetics of solute adsorption at heterogeneous solid/solution interfaces: On the possibility of distinguishing between the diffusional and the surface reaction kinetics models, Appl. Surf. Sci. 253 (2007) 5827–5840.
[10] W. Rudzinski, W. Plazinski, Kinetics of dyes adsorption at the solid−solution interfaces: A theoretical description based on the two-step kinetic model, Environ. Sci. Technol. 42 (2008) 2470–2475.
[11] S. Azizian, H. Bashiri, H. Iloukhani, Statistical rate theory approach to kinetics of competitive adsorption at the solid/solution interface, J. Phys. Chem. C 112 (2008) 10251–10255.
[12] S. Lagergren, About the theory of so-called adsorption of soluble substances, K. Sven. Vetenskapsakad. Handl. 24 (1898) 1–39.
[13] J. Sobkowski, A. Czerwiński, Kinetics of carbon dioxide adsorption on a platinum electrode, J. Electroanal. Chem. Interfacial Electrochem. 55 (1974) 391–397.
[14] W. Rudzinski, W. Plazinski, Kinetics of solute adsorption at solid/solution interfaces: A theoretical development of the empirical pseudo-first and pseudo-second order kinetic rate equations, based on applying the statistical rate theory of interfacial transport, J. Phys. Chem. B 110 (2006) 16514–16525.
[15] Y.J. Tu, C.F. You, Phosphorus adsorption onto green synthesized nano-bimetal ferrites: Equilibrium, kinetic and thermodynamic investigation, Chem. Eng. J. 251 (2014) 285–292.
[16] P. Ganesan, R. Kamaraj, S. Vasudevan, Application of isotherm, kinetic and thermodynamic models for the adsorption of nitrate ions on graphene from aqueous solution, J. Taiwan Inst. Chem. Eng. 44 (2013) 808–814.
[17] J. Shen, Z. Duvnjak, A reversible surface reaction model with an effectiveness factor and its application to sorption kinetics of cupric ions on corncob particles, Sep. Purif. Technol. 44 (2005) 69–77.
[18] A. Özer, Removal of Pb(II) ions from aqueous solutions by sulphuric acid-treated wheat bran, J. Hazard. Mater. 141 (2007) 753–761.
[19] A.W. Marczewski, Kinetics and equilibrium of adsorption of organic solutes on mesoporous carbons, Appl. Surf. Sci. 253 (2007) 5818–5826.
[20] D. Karadag, Y. Koc, M. Turan, M. Ozturk, A comparative study of linear and non-linear regression analysis for ammonium exchange by clinoptilolite zeolite, J. Hazard. Mater. 144 (2007) 432–437.
[21] A.W. Marczewski, Application of mixed order rate equations to adsorption of methylene blue on mesoporous carbons, Appl. Surf. Sci. 256 (2010) 5145–5152.
[22] E. Guibal, Interactions of metal ions with chitosan-based sorbents: A review, Sep. Purif. Technol. 38 (2004) 43–74.
[23] N. Li, R. Bai, C. Liu, Enhanced and selective adsorption of mercury ions on chitosan beads grafted with polyacrylamide via surface-initiated atom transfer radical polymerization, Langmuir 21 (2005) 11780–11787.

[24] J. Ma, Y. Shen, C. Shen, Y. Wen, W. Liu, Al-doping chitosan–Fe(III) hydrogel for the removal of fluoride from aqueous solutions, Chem. Eng. J. 248 (2014) 98–106.
[25] Y.S. Ho, Second-order kinetic model for the sorption of cadmium onto tree fern: A comparison of linear and non-linear methods, Water Res. 40 (2006) 119–125.
[26] N. Viswanathan, S. Meenakshi, Selective sorption of fluoride using Fe(III) loaded carboxylated chitosan beads, J. Fluorine Chem. 129 (2008) 503–509.
[27] F. Raji, M. Pakizeh, Kinetic and thermodynamic studies of Hg(II) adsorption onto MCM-41 modified by $ZnCl_2$, Appl. Surf. Sci. 301 (2014) 568–575.